Chinese Chemical Letters 34 (2023) 108269

Contents lists available at ScienceDirect

Chinese Chemical Letters

journal homepage: www.elsevier.com/locate/cclet

Well-dispersed Mn/g-C_3N_4 as bifunctional catalysts for selective epoxidation of olefins and carbon dioxide cycloaddition☆

Minxing Du[a,b,1], Yuxia Sun[a,1], Jiaojiao Zhao[a], Haiyan Hu[a,b], Liwei Sun[a], Yuehui Li[a,*]

[a] State Key Laboratory for Oxo Synthesis and Selective Oxidation, Suzhou Research Institute of LICP, Center for Excellence in Molecular Synthesis, Lanzhou Institute of Chemical Physics (LICP), Chinese Academy of Sciences, Lanzhou 730000, China
[b] University of Chinese Academy of Sciences, Beijing 100049, China

ARTICLE INFO

Article history:
Received 18 October 2022
Revised 7 February 2023
Accepted 23 February 2023
Available online 28 February 2023

Keywords:
Well-dispersed Mn catalyst
Bifunctional catalyst
Epoxidation
CO_2
Cycloaddition

ABSTRACT

Epoxidation is an important chemical process for the production of epoxides, key building blocks in chemical industry. Despite great efforts being made to facilitate this process, it remains a significant challenge to develop cost-effective, environmental-friendly, and selective catalysts. Herein, we reported a highly dispersed Mn supported by g-C_3N_4 (Mn/g-C_3N_4) with Mn loading up to 2.56 wt%. The Mn/g-C_3N_4 exhibited satisfied catalytic performance for olefin epoxidation with excellent conversion (91%), high selectivity (93%) as well as outstanding recycling stability. Further analysis revealed the importance of Mn-N structure for the generation of active oxo-containing species and subsequent oxygen atom transfer. Besides, an efficient synthesis of cyclic carbonates from styrene epoxide and CO_2 has been achieved (88% conversion, 89% selectivity) based on the polar Mn-N coordinated characteristics of Mn/g-C_3N_4 catalyst.

Epoxides are important intermediates in the synthesis of various kinds of fine chemicals, pharmaceuticals, perfumes, and polymers [1–4]. For example, the cycloaddition of epoxides with CO_2 produces cyclic carbonates [5,6], which are widely adopted as solvent in lithium batteries and monomer for the preparation of polycarbonates [7]. Epoxidation of olefins is a straightforward method for epoxide synthesis [8–11]. In view of the key role of epoxides in the chemical industry, it is highly desired to develop efficient and green epoxidation processes.

In this respect, Au [12–14], Ag [15–17], Co [18,19], Fe [20], Mo [21,22], Ce [23] and Mn [24] based catalysts have been employed in the epoxidation of alkenes [25,26]. Heterogeneous catalysts, such as Ag/α-Al_2O_3 [27] and gold nanoparticles supported on layered double hydroxide were also reported to be efficient catalysts for the epoxidation of styrene [28]. In transition metal-based catalysts, the heme-like structures constitute an important part, with the metal-N4 site as the catalytic center, since the understanding of cytochrome P450 function in 2000 [29]. However, it was found that metal-N4 complexes (*e.g.*, Fe-Porphyrin, Mn-Phthalocyanine) [30,31] went through dimerization and deactivation under oxidative reaction conditions. This issue limited their further applications.

In recent decades, various heterogeneous catalysts containing heme-like structures, adopting immobilization [32,33] or crosslinking strategy [34,35] were reported. These heterogenization methods improved the stability of catalysts. On the other hand, the metal-N4 site could be constructed by the coordination of metal on the N-contained supports. Typically, single-atom catalysts could be obtained by pyrolysis of nitrogenous precursors in the presence of metal precursors at elevated temperatures to construct well-dispersed metal centers on N-contained support, *e.g.*, C_3N_4 [36]. In principle, these systems could maximize the catalytic performance. In this term, the Ag-C_3N_4 [26], as well as the Fe_2-C_3N_4 [37] were developed with good epoxidation activity. However, other transition metals were rarely investigated in the target epoxidation as well as the subsequent cyclic addition with CO_2 to cyclocarbonates.

Herein, the well-dispersed Mn catalyst supported on nitrogen-rich g-C_3N_4 (Mn/g-C_3N_4) was firstly adopted in the epoxidation and subsequent CO_2 cycloaddition. The Mn/g-C_3N_4 exhibits excellent performance in the epoxidation of aromatic olefins (up to 91% conversion, 93% selectivity), and the cycloaddition of styrene epoxide and CO_2 to carbonates (88% conversion, 89% selectivity in the presence of ammonium salts). Moreover, it was inferred that the Mn-N site catalyzes the epoxidation by oxygen transferring from Mn-O species to the olefin, formed *via* the first *t*BuOOH addition

☆ Dedication to Prof. Lixin Dai on the Occasion of His Centenary Birthday.

* Corresponding author.
E-mail address: yhli@licp.cas.cn (Y. Li).

[1] These authors contributed equally to this work.

https://doi.org/10.1016/j.cclet.2023.108269
1001-8417/

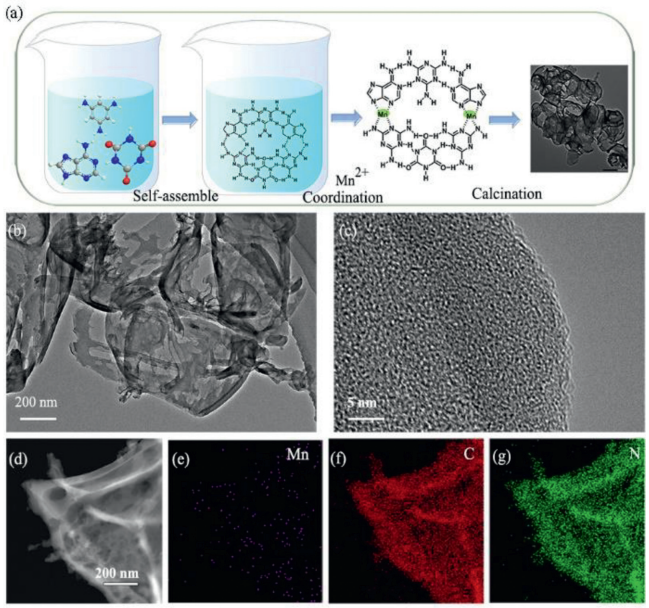

Fig. 1. (a) Schematic illustration of the preparation of well-dispersed Mn/g-C_3N_4. (b) TEM image, (c) HRTEM image, (d) HAADF-STEM image, and corresponding EDX elemental mapping of Mn (e), C (f), N (g) of Mn/g-C_3N_4(3).

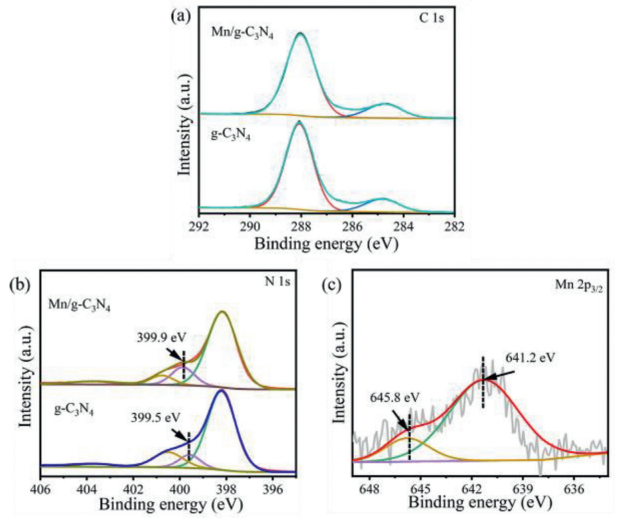

Fig. 2. High-resolution XPS spectra of (a) C 1s, (b) N 1s, (c) Mn 2p regions for Mn/g-C_3N_4(3).

to the Mn-N site and followed by the heterolytic cleavage of the *t*BuOO-Mn-N site. Furthermore, the catalyst was applied to promote the sequent cycloaddition of the epoxides with CO_2. This thus provided a new and high-yield heterogeneous system to synthesize cyclic carbonates from olefins.

The highly-dispersed Mn supported on pyrrolic N-rich graphitic carbon nitride (Mn/g-C_3N_4) was synthesized *via* an impregnation-calcination method (Fig. 1a). First, melamine (M), cyanuric acid (CA), and adenine (A) were self-assembled in a homogeneous system *via* hydrogen bonding. Then Mn^{2+} coordinated with the self-assembled polymer. Finally, the well-dispersed Mn/g-C_3N_4 was obtained by calcination of Mn^{2+} loaded polymer in the N_2 atmosphere (see details in the Experimental Section in Supporting information).

The crystalline structure of the obtained g-C_3N_4 and Mn/g-C_3N_4 materials were first examined by X-ray diffraction (XRD). As shown in Fig. S1 (Supporting information), the patterns of g-C_3N_4 and Mn/g-C_3N_4(3), showed a high degree of resemblance, both characterized by a dominant peak at $2\theta = 27.4°$ corresponding to the (002) interlayer reflection of a graphitic structure, as well as a weak diffraction peak at about 13°, attributed to the in-plane repeating units of heptazine [38].

Notably, typical diffraction peaks of Mn species (either metallic or oxides) were not observed, further eliminating the existence of Mn-containing crystalline species and indicating the high dispersion of Mn in the g-C_3N_4 framework. In addition, the Fourier transform infrared (FT-IR) spectra of g-C_3N_4, and Mn/g-C_3N_4(3) (Fig. S2 in Supporting information) evidences the condensed aromatic C–N–C networks [39]. The band at 808 cm^{-1} together with the bands in the range of 1100–1600 cm^{-1} were present, attributed to the breathing mode of tri-*s*-triazine units and the stretching modes of C–N heterocycles.

The high-resolution transmission electron microscope (HRTEM) was further employed to determine the morphology of the prepared catalyst. As shown in Figs. 1b and c, and Fig. S4 (Supporting information), g-C_3N_4 and Mn/g-C_3N_4(3) displayed a curved and flake-like structure. No nanoparticles were observed in the transmission electron microscopy (TEM) as well as high-resolution TEM (HR-TEM) images, supporting the high degree of Mn dispersion. The corresponding energy-dispersive X-ray spectroscopy (EDX) mapping images (Figs. 1e-g) reveal that Mn, C, and N elements are homogeneously distributed in the entire g-C_3N_4 framework. Furthermore, the quantitative measurement by inductively coupled plasma mass spectrometry (ICP-MS) indicates ~2.56 wt% manganese was implanted in the catalyst.

The chemical compositions and electronic configurations of the as-synthesized Mn/g-C_3N_4(3) catalyst were characterized by X-ray photoelectron spectroscopy (XPS). For C 1s spectra in g-C_3N_4 and Mn/g-C_3N_4(3) (Fig. 2a), two distinct peaks at 284.8 eV and 288.0 eV are observed, attributed to sp^2 C–C bonds and sp^2 hybridized carbon in N-containing aromatic ring (N–C=N) [40,41]. The observed N 1s spectra of Mn/g-C_3N_4(3) (Fig. 2b) was deconvoluted into four fitted peaks located at around 398.2, 399.9, 400.4, and 403.7 eV, respectively. These peaks are attributed to pyridinic N, pyrrolic N, graphitic N, and π-excitations, respectively [42,43]. Compared with pure g-C_3N_4, the binding energy of pyrrolic N in Mn/g-C_3N_4(3) shifts up by 0.4 eV to 399.9 eV, suggesting that the pyrrolic N is most likely to provide coordination sites for Mn atoms to form Mn-Nx moieties. The Mn 2p spectra of Mn/g-C_3N_4(3) was displayed in Fig. 2c, with one strong peak at 641.2 eV as well as a satellite peak at 645.8 eV detected. The characteristic feature of Mn $2p_{3/2}$ peak for Mn/g-C_3N_4(3) is close to that of Mn^{II}, suggesting that the valence state of the Mn species in Mn/g-C_3N_4(3) is +2 [36].

We investigated the catalytic performance of as-prepared catalysts for epoxidation of the model substrate styrene. The conversion of styrene and the selectivity of products are shown in Fig. 3. Using TBHP (5.0~6.0 mol/L in decane) as the oxidant, the Mn/g-C_3N_4(3) sample shows unique and superior catalytic performance (91% conversion, 93% selectivity) toward epoxidation without any additives, along with trace benzaldehyde. Comparatively, when g-C_3N_4 was adopted as the catalyst, the catalytic activity was quite poor, with only 14% styrene oxide obtained. Thus, the well-dispersed Mn played a non-negligible role in the epoxidation. The content of N in Mn/g-C_3N_4 was optimized by varying the molar ratio of $MnCl_2$ to adenine in the Mn/CA-A-M precursor. With N content increasing, the yield of styrene oxide showed a volcano shape following this order: Mn/g-C_3N_4(3) (85%) > Mn/g-C_3N_4(1) (56%) > Mn/g-C_3N_4(6) (39%). Furthermore, the prepared Mn NPs/g-C_3N_4(3) and $MnCl_2$ were applied in the epoxidation of styrene. By contrast, only trace or 14% yields of the epoxide were presented. These combined revealed the importance of well-dispersion of Mn and g-C_3N_4 framework in the epoxidation.

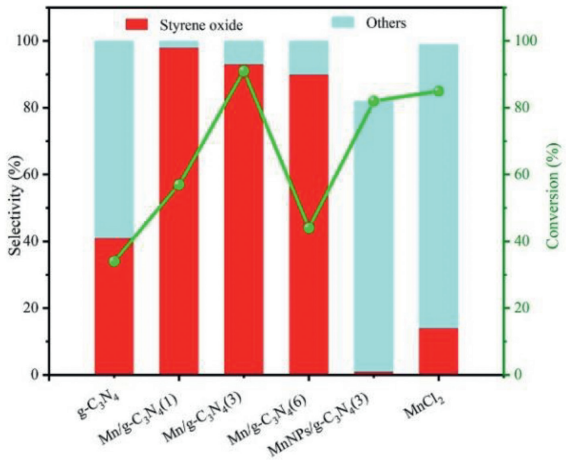

Fig. 3. Catalytic activities for selective oxidation of styrene. Reaction condition: styrene (0.5 mmol), Cat. (7.0 mg), TBHP (5~6 mol/L in decane) (2 equiv.), solvent (2 mL), 100 °C, 8 h. Conversion and selectivity were determined by GC analysis using dodecane as the internal standard.

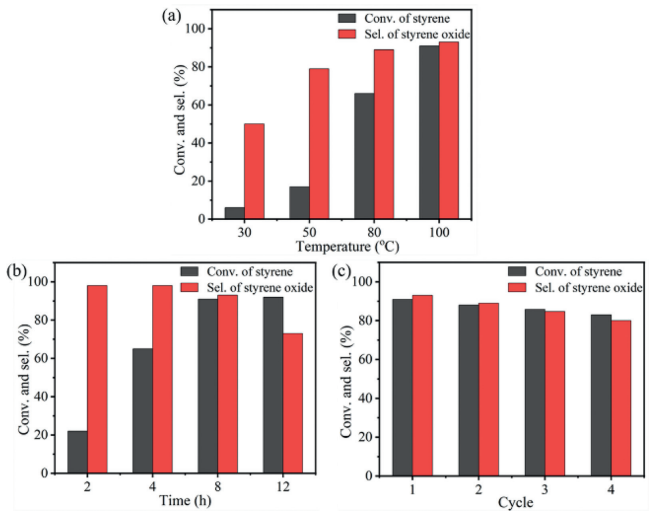

Fig. 4. Effect of temperature (a) and reaction time (b) on Mn/g-C_3N_4(3) catalyzed epoxidation of styrene. (c) Recycle test of Mn/g-C_3N_4(3) for epoxidation of styrene. Reaction conditions: styrene (0.5 mmol), Mn/g-C_3N_4(3) (0.65 mol%), TBHP (2 equiv.), DCE (2 mL), 100 °C and 8 h.

In addition, various oxidants, such as TBHP, O_2, and H_2O_2 were screened. The catalytic activities of these oxidants toward styrene epoxidation are illustrated in Supporting information (Table S3, entries 1–3). Compared with TBHP, both O_2 and H_2O_2 showed inferior catalytic activity under same experimental conditions (trace to 4%). Therefore, TBHP was chosen as the oxidant for the epoxidation of styrene catalyzed by Mn/g-C_3N_4(3). Afterwards, the catalytic epoxidation using different solvents was investigated and the results are present in entries 4–6 (Table S3). The yields obtained were in the order DCE > MeCN > Heptane > EtOH, indicating that DCE is the optical solvent.

The influence of reaction temperature is shown in Fig. 4a. The conversion showed a steep increase from 6% to 91%, along with the increase of selectivity of styrene oxide from 50% to 93%, when the temperature increases from 30 °C to 100 °C. Further increasing the reaction temperature to higher than 100 °C, the decomposition of TBHP might proceed prior to the target oxidation, which led to a decrease in the styrene conversion. Fig. 4b showed the variation in conversion and selectivity with time. In the range of 2–8 h, the conversion increases rapidly from 22% to 92%. Further extending the reaction time to 12 h results in an obvious decrease in the selectivity from 93% to 73%, owing to the side reaction of styrene oxide.

In addition, the effect of catalyst/styrene mole ratios on the styrene epoxidation was investigated (Fig. S7a). The selectivity slightly increased with the increasing dosage of Mn/g-C_3N_4(3), up to 94% obtained with 2.5 mol% of catalyst. The effect of TBHP/styrene ratio on epoxidation was further examined (Fig. S7b). As the molar ratio increased to 2, the conversion increases rapidly from 25% to 91%. Thus, the optimum conditions can be summarized as follows: Mn/g-C_3N_4(3) (0.65 mol%), TBHP (2 equiv.), 100 °C, 8 h.

The benefit of a heterogeneous catalyst compared to a homogeneous one is its easy separation and recycling. The stability of the catalyst was tested by four-time recycling under the same reaction conditions. As shown in Fig. 4c, the catalyst could be reused without significant loss of reactivity and selectivity. Moreover, the ICP-MS result showed that less than 0.3 ppm Mn ions were detected in the supernatant fluid after centrifugation, indicating good stability of the catalyst. Meanwhile, to probe the near-surface electronic structure of recovered Mn/g-C_3N_4(3), XPS spectra was collected (Fig. S5b). It was observed that the intensities of the Mn 2p3/2 peak at 641.2 eV as well as the satellite peak at 645.8 eV attributed to Mn (II) were slightly lower than the pristine sample, demonstrating that the local Mn center on the surface went through limited changes. This might be explained by possible oxidation of Mn^{II} to Mn^{III} in the presence of oxidant.

To test the substrate scope of Mn/g-C_3N_4(3), a series of aromatic olefins with different substituents were screened under identical conditions. The results are presented in Scheme 1. Various mono-substituted styrene with either electron-donating or electron-withdrawing groups were converted with moderate to good yields (**2a-2i**). In general, higher selectivity and yields were obtained for electro-deficient substrates, except for substitution by NO_2 group (**2g**, 43% yield) or *othro*-substitution (**2h-2i**, 39%–41% yields). While for the aliphatic alkenes, only trace amounts of desired products were detected (**2j** and **2k**).

Furthermore, in terms of the development of carbon dioxide as C1 building block in the synthesis of valuable chemicals, synthesis of cyclic carbonates from styrene epoxide and CO_2 has been explored using the same catalyst. Styrene-derived carbonate was

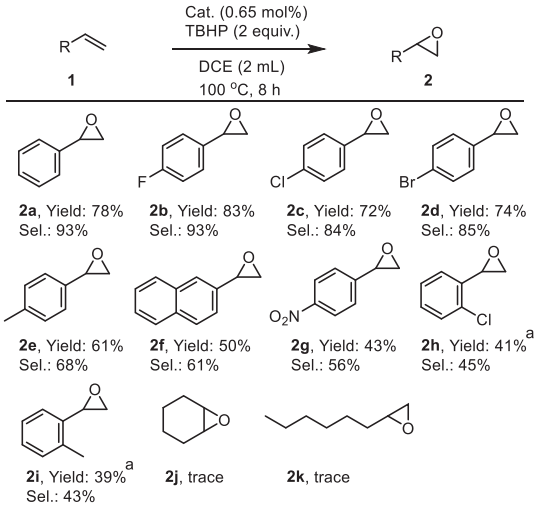

Scheme 1. Chemical epoxidation of different alkenes with Mn/g-C_3N_4(3) catalyst. Reaction conditions: Olefin (0.5 mmol), Cat. (0.65 mol%), TBHP (2 equiv.), DCE (2 mL), 100 °C, 8 h. Isolated yields. [a] NMR yield. Selectivity of **2** determined by NMR analysis using 1,1,2,2-tetrachloroethane as the internal standard.

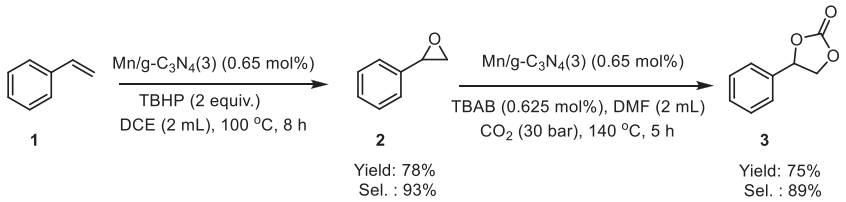

Scheme 2. Two-steps synthesis of styrene carbonate. Reaction conditions: (1) styrene (0.5 mmol), (2) styrene epoxidation (1 mmol). Isolated yields. Selectivity of **2** and **3** determined by GC analysis using dodecane as the internal standard.

afforded with 88% conversion of styrene epoxide and 89% selectivity, as shown in Scheme 2 and Table S4 (Supporting information). The activity might originate from the basicity of C_3N_4 and the Lewis acidic Mn site. To better clarify the role of Mn-C_3N_4(3) in CO_2 cycloaddition, the strength of the basic and acidic sites on the catalyst were assessed by CO_2-TPD (temperature programmed desorption) and NH_3-TPD. As shown in the CO_2-TPD profile (Fig. S8 in Supporting information), the main peak around 207 °C indicated the presence of weak basic sites, while the small peaks around 378∼460 °C correspond to medium basicity of Mn/g-C_3N_4. Besides, the main peak around 211 °C in the NH_3-TPD signal suggested weak acidic sites. According to previous studies [44], the catalyst combined with acidity and basicity could effectively promote the activation of both CO_2 and epoxides. These combined elucidated the bifunctional role of Mn/g-C_3N_4(3) in epoxidation as well as CO_2 cycloaddition.

To further verify the important role of the highly dispersed Mn-N site in epoxidation, the poisoning experiment using KSCN was carried out. Normally, SCN^- can strongly bind to metal centers. The strong coordination enables the block of metal sites. As shown in Scheme S1 (Supporting information), after the addition of SCN^-, the yield of styrene oxide decreases from 85% to trace along with a significantly lower conversion. Therefore, Mn-Nx sites should play a predominant role in the catalytic process.

Moreover, in Mn-based homogeneous catalytic systems, Mn(IV)-oxo species have been frequently reported as the active intermediate in the epoxidation of olefins [45,46]. As a heterogeneous model of Mn-Nx in the Mn/g-C_3N_4(3) framework, Mn-alkyl peroxo species could be facially formed after activation of the peroxide by manganese center. The possible mode of MnO–O cleavage was investigated adopting cumyl hydroperoxide (CHP) probe. The resulting products of the probe reaction could help identify the homolytic or heterolytic cleavage pathway of MnO–O bond [47,48]. As demonstrated in Scheme S2 (Supporting information), cumyl alcohol directs to the heterolytic O–O bond cleavage, with acetophenone corresponding to homolytic O–O bond cleavage. Compared to the results without catalyst, cumyl alcohol was found to be the major product in the system catalyzed by Mn/g-C_3N_4, which directed to a heterolytic O–O bond cleavage. Based on the results, a possible reaction mechanism was inferred as Scheme S3 (Supporting information). The Mn-Nx site catalyzes the epoxidation by oxygen transfer between the olefin and Mn-O species, which is formed *via* the ^{t}BuOOH addition to the Mn-N site and followed by the heterolytic cleavage of the *t*BuOO-Mn-N site.

In summary, inspired by the bio-enzyme (cytochrome P450) catalytic systems for the epoxidation of olefins and the fact that well-dispersed active centers can maximize the catalytic performance, we have synthesized highly-dispersed Mn/g-C_3N_4 materials. The as-prepared Mn/g-C_3N_4 catalyst exhibits good catalytic performance for olefin epoxidation with excellent conversion (up to 91%), high selectivity (up to 93%), broad substrate scope as well as outstanding cyclic stability. Furthermore, the catalysts were utilized to promote the cycloaddition of the epoxides with CO_2, laying foundations for a promising industrial process of environmentally benign chemical fixation of CO_2.

Declaration of competing interest

The authors declare that they have no known competing financial interests or personal relationships that could have appeared to influence the work reported in this paper.

Acknowledgments

We are grateful for the financial supports from the National Natural Science Foundation of China (Nos. 21633013 and 22102197), Jiangsu Province Natural Science Foundation (No. BK20211096) and the Science Fund of Shandong Laboratory of Advanced Materials and Green Manufacturing (Yantai, No. AMGM2021F07).

Supplementary materials

Supplementary material associated with this article can be found, in the online version, at doi:10.1016/j.cclet.2023.108269.

References

[1] A.S. Sharma, V.S. Sharma, H. Kaur, R.S. Varma, Green Chem. 22 (2020) 5902–5936.
[2] K. Kamata, K. Yonehara, Y. Sumida, et al., Science 300 (2003) 964–966.
[3] C. Ge, C. Chen, Green Synth. Catal. (2022), doi:10.1016/j.gresc.2022.07.005.
[4] H. Wang, S. Gu, Q. Yan, L. Ding, F.E. Chen, Green Synth. Catal. 1 (2022) 12–15.
[5] T. Sakakura, K. Kohno, Chem. Commun. 11 (2009) 1312–1330.
[6] J. Liu, G. Yang, Y. Liu, et al., Green Chem. 22 (2020) 4509–4515.
[7] I. Kim, M.J. Yi, K.J. Lee, et al., Catal. Today 111 (2006) 292–296.
[8] X. Song, D. Hu, X. Yang, et al., ACS Sustain. Chem. Eng. 7 (2019) 3624–3631.
[9] Y. Wu, X. Tang, J. Zhao, et al., ACS Sustain. Chem. Eng. 8 (2020) 1178–1184.
[10] J. Lin, F. Wang, J. Tian, et al., Chin. Chem. Lett. 33 (2022) 1515–1518.
[11] X.T. Zhou, H.Y. Yu, Y. Li, H.B. Wu, H.B. Ji, Chin. Chem. Lett. 34 (2003) 107658.
[12] T. Hayashi, K. Tanaka, M. Haruta, J. Catal. 178 (1998) 566–575.
[13] Y. Liu, C. Zhao, B. Sun, H. Zhu, W. Xu, Appl. Catal. A 624 (2021) 118329.
[14] X.Y. Chen, S.L. Chen, A.P. Jia, J.Q. Lu, W.X. Huang, Appl. Surf. Sci. 393 (2017) 11–22.
[15] Y. Lei, F. Mehmood, S. Lee, et al., Science 328 (2010) 224–228.
[16] A.J.F. Von Hoof, I.A.W. Filot, H. Friedrich, E.J. Hensen, ACS Catal. 8 (2018) 11794–11800.
[17] X. Zhang, G. Kumari, J. Heo, P.K. Jain, Nat. Commun. 9 (2018) 3056.
[18] R.V. Jagadeesh, H. Junge, M.M. Pohl, et al., J. Am. Chem. Soc. 135 (2013) 10776–10782.
[19] D. Banerjee, R.V. Jagadeesh, K. Junge, et al., Angew. Chem. Int. Ed. 53 (2014) 4359–4363.
[20] D. Malko, Y. Guo, P. Jones, G. Britovsek, A. Kucernak, J. Catal. 370 (2019) 357–363.
[21] C.I. Fernandes, N.U. Silva, P.D. Vaz, T.G. Nunes, C.D. Nunes, Appl. Catal. A 384 (2010) 84–93.
[22] Y. Kuwahara, N. Furuichi, H. Seki, H. Yamashita, J. Mater. Chem. A 5 (2017) 18518–18526.
[23] J. Ren, X. Liu, R. Gao, W.L. Dai, J. Energy Chem. 26 (2017) 681–687.
[24] Y. Zhang, H. Li, L. Zhang, R. Gao, W.L. Dai, ACS Sustain. Chem. Eng. 7 (2019) 17008–17019.
[25] B.S. Lane, K. Burgess, Chem. Rev. 103 (2003) 2457–2474.
[26] S. Tian, C. Peng, J. Dong, et al., ACS Catal. 11 (2021) 4946–4954.
[27] A.J.F. Von Hoof, E.A.R. Hermans, A.P. van Bavel, H. Friedrich, E.J.M. Hensen, ACS Catal. 9 (2019) 9829–9839.
[28] F. Zhang, X. Zhao, C. Feng, et al., ACS Catal. 1 (2011) 232–237.
[29] I. Schlichting, J. Berendzen, K. Chu, et al., Science 287 (2000) 1615–1622.
[30] M.H. Alkordi, Y. Liu, R.W. Larsen, J.F. Eubank, M. Eddaoudi, J. Am. Chem. Soc. 130 (2008) 12639–12641.
[31] I. Ahmad, S.R. Shagufta, Tetrahedron 104 (2022) 132604.
[32] Z. Han, X. Han, X. Zhao, J. Yu, H. Xu, J. Hazard. Mater. 320 (2016) 27–35.

[33] S. Chen, W. Xie, B. Guo, T. Pan, W. Chen, Cellulose 26 (2019) 7863–7875.
[34] B. Wang, J. Lin, Q. Sun, C. Xia, W. Sun, ACS Catal. 11 (2021) 10964–10973.
[35] T. Maschmeyer, F. Rey, G. Sankar, J.M. Thomas, Nature 378 (1995) 159–162.
[36] J. Feng, H. Gao, L. Zheng, et al., Nat. Commun. 11 (2020) 4341.
[37] S. Tian, Q. Fu, W. Chen, et al., Nat. Commun. 9 (2018) 2353.
[38] X. Wang, K. Maeda, A. Thomas, et al., Nat. Mater. 8 (2009) 76–80.
[39] B. Wu, L. Zhang, B. Jiang, et al., Angew. Chem. Int. Ed. 60 (2021) 4815–4822.
[40] Q. Lin, L. Li, S. Liang, et al., Appl. Catal. B 163 (2015) 135–142.
[41] J. Li, B. Shen, Z. Hong, et al., Chem. Commun. 48 (2012) 12017–12019.
[42] J.C. Wang, H.C. Yao, Z.Y. Fan, et al., ACS Appl. Mater. Interfaces 8 (2016) 3765–3775.
[43] F. Chen, X.L. Wu, C. Shi, et al., Adv. Funct. Mater. 31 (2021) 2007877.
[44] J. Liu, Y.Liu G.Yang, et al., Green Chem. 22 (2020) 4509–4515.
[45] M. Guo, J. Zhang, L. Zhang, et al., J. Am. Chem. Soc. 143 (2021) 18559–18570.
[46] N. Sharma, H.B. Zou, Y.M. Lee, S. Fukuzumi, W. Nam, J. Am. Chem. Soc. 143 (2021) 1521–1528.
[47] C. Miao, B. Wang, Y. Wang, et al., J. Am. Chem. Soc. 138 (2016) 936–943.
[48] J. Du, C. Miao, C. Xia, et al., ACS Catal. 8 (2018) 4528–4538.